OPEN ACCESS

Research Article

In vitro and in vivo evaluation of nano-composite hydrogels of *Heliotropium indicum* extract for wound healing

Satish C S

Department of Pharmaceutics PES College of Pharmacy, 50 Feet Road, Hanumanthanagar, Bangalore-570050, India

Abstract: *Background:* Wound infection is a manifestation of disturbed host–bacteria equilibrium in a traumatized tissue environment in favor of the bacteria. A wound infection not only has the possibility to elicit a systemic response (sepsis), but is highly likely to inhibit the multiple processes. *Materials and Methods:* Solid lipid nanoparticles (SLNs) were prepared using glycerol tristearate and poloxamer by solvent evaporation method. The particle size, polydispersity index (PDI), zeta potential (ZP), FTIR, NMR, water vapor transmission rate determination and in vivo wound healing studies were performed. *Results:* The average particle size results showed that the nanoparticle size of N2 was in the range of 0.4-0.8 μm and polydispersivity index less than 1. The prepared hydrogels had WVTR in the range of 2187.9 g/m^2 to 2954 g/m^2 could maintain a suitable moist environment in the wound that could enhance the wound contraction and tissue regeneration, thereby accelerating wound healing. Heliotropium indicum extract SLN Hydrogel significantly contributed to wound healing compared with the blank control group at 15 and 18 day post-wounding ($P < 0.05$). *Conclusion:* Nanoparticle containing Heliotropium indicum extract could be released slowly from Carboxymethyl chitosan oxidized alginate hydrogel hydrogel in a sustained manner to stimulate fibroblast proliferation, capillary formation and collagen production that can significantly effect on the healing phases. As a result, we suggested that the prepared hydrogel might have great potential application in the wound healing.

Keywords: Nanoparticle, wound healing, hydrogel.

1. INTRODUCTION

The healing of skin wound is a complex process requiring the collaborative efforts of many different tissues and cell lineages. Wound healing process results in the contraction and closure of wound tissue and also it restores functional barrier (Martin, P. 2007). Four overlapping steps are involved in dermal wound healing. These steps are the inflammatory phase (occur immediately after wound is formed), the migratory, proliferative and maturation phase resulting in remodeling (Patrulea, V. *et al*., 2015). Regarding the other factors involved in wound healing, the extracellular matrix (ECM) has a key role in orchestrating and guiding cell phenotype, adhesion, migration and proliferation (Dreifke, M.B. *et al*., 2015). The ECM comprises proteins synthesized by fibroblasts, including proteoglycans (e.g., chondroitin sulfate), keratin sulfate, heparin sulfate and fibrous proteins like laminin, type IV collagen and elastin. In addition, the ECM serves as a deposit for growth factors, proteases, cytokines and chemokines (Hynes, R.O. *et al*., 2009, Rodrigues, M. *et al*., 2019).

Chitosan (CS), as a semi-crystalline aminopolysaccharide obtained by deacetylation of chitin (Sultankulov, B. *et al*., 2019) a naturally occurring polysachharide, has been widely used in biomedical and pharmaceutical field owing to its favorable properties such as nontoxicity, excellent biocompatibility (Jacob, B. *et al*., 2019) biodegradability. Review of literature yields a large number of studies have been performed on chitosan-based drug delivery systems including films (Patrulea, V. *et al*., 2019) for wound healing application (Abbas, M. *et al*., 2019)

The use of chitosan in drug delivery is limited due to its poor solubility at physiological pH, which in turn decreases efficiency of drug delivery below *p*H 6 (Sieval, A. B. *et al*., 1998). In this view, several methods were investigated to improve chitosan solubility. The most preferred approach to increase chitosan solubility at neutral pH is to introduce permanent charges into the chitosan backbone. In order to obtain a water-soluble chitosan derivative, Domard et al prepared quaternized chitosan through methylation (Domard, A. *et al.,* 1986), while Chen and Park

developed carboxymethylated chitosan (Chen, X.G., *et al.,* 2003). Carboxymethyl chitosan is a water soluble derivative of chitosan which has been successfully used as biomaterial in both research and clinical applications. Carboxymethyl chitosan possess favorable biocompatibility, no antigenicity, moisture retention, specific bioadhesion, and antibacterial ability. Chitosan and Carboxymethyl chitosan are widely regarded as one of the attractive materials for developing wound healing agents (Liu Q. *et al.,* 2017).

Carboxymethyl chitosan is prepared by the introduction of a carboxymethyl group from chloroacetic acid to the -OH and -NH₂ groups in chitosan. This results in an increase in the water solubility and pH sensitivity of carboxymethyl chitosan, making it a widely used chitosan derivative in the biomedical field (Upadhyaya, L. *et al.,* 2013). It is highly soluble in neutral and alkaline solutions and exhibits better sensitivity (Chen, X.G. *et al.,* 2003), biocompatibility, biodegradability, and moisture-retaining capacity than chitosan alone (Chen, L.Y. *et al.,* 2003). Moreover, its chemotaxis to neutrophils and macrophages helps prevent wound infection in early healing and is beneficial to granulation tissue formation (Zhu, X. *et al.,* 2005) and epidermal cell regeneration in late healing (Chen, X.G. *et al.,* 2002). In addition, carboxymethyl chitosan has been reported to inhibit the formation of algogenic substances, such as histamine, serotonin, and bradykinin, as well as prevent scar formation and promote normal fibrocyte growth (Lu, G. *et al.,* 2007). Previous studies have shown that carboxymethyl chitosan stimulates the macrophage release of L929 cell growth factor, and living autologous cells subsequently stimulate the migration of L929 and other wound healing cells under the regulation of growth factors and bioactive substances (Min, S.K. *et al.,* 2007). Solid lipid nanoparticles (SLNs) can be used on damaged or inflamed skin as they are composed of non-irritant and nontoxic lipids and efficacy of entrapped drug has been enhanced as reported in the literature.

The present work aims to evaluate SLN with glycerol tristearate as encapsulating matrix of Heliotropium indicum, in hydrogel of carboxymethyl chitosan and oxidised sodium alginate for topical wound application both in vitro and in vivo

2. MATERIALS AND METHODS

2.1. Materials

Chitosan (Deacetylation content of 88.2%) was purchased from Himedia, India. glycerol tristearate, sodium alginate were purchased from Himedia, India. Monochloroacetic acid, acetic acid, isopropanol, sodium periodate, ethylene glycol, sodium chloride, sodium hydroxide and methanol were all were purchased from Himedia, India and used without further purification. Heliotropium indicum extract was gift sample from S.A. Herbal Bioactives LLP, Mumbai.

2.2 Preparation of SLNs

SLNs were prepared by the method reported in literature (Shah, M. *et al.,* 2012). In 5 ml of ethanol, Glycerol tristearate was dissolved and Heliotropium indicum extract was dispersed in the ethanol solution. The poloxamer 188 in water was placed on a magnetic stirrer, and the Glycerol tristearate and Heliotropium indicum extract mixture was dispersed dropwise into the water phase containing poloxamer at a stirring speed of 1000 rpm at 80°C. After stirring for 1 h, the resultant emulsion was cooled by adding ice-cold water to solidify the nanoparticles, centrifuged at 3000 rpm to remove unentrapped Heliotropium indicum extract, and then centrifuged again at 6,000 rpm for 30 min at 4°C. This was done to remove the free drug. The resultant solid mass was stored for further studies. The amount of lipid, drug and surfactant were varied in the preparation of nanoparticles (Table 1).

2.3 Evaluation of SLNs
2.3.1 Particle Size Analysis and Zeta Potential determination

The particle size and polydispersivity index of the optimized formulation was measured by dynamic light scattering (DLS Horiba scientific SZ-100 series) after equilibration for 2 mins (Merisko-Liversidge, E. *et al.,* 2004). The cell temperature was 25°C; and the scattering angle was 90°.

Zetasizer (Malvern Instruments Ltd, Worcs, UK) equipped with the Malvern PCS software (version 1.27) was used for Zeta potential measurement. A required amount of the sample was diluted with 5 mL of deionized water and placed into the electrophoretic cell of the instrument, where a potential of ±150 was applied. All analyses were done in triplicate (Pignatello, R. *et al.,* 2006).

2.3.3 Preparation of Carboxymethyl chitosan from Chitosan

Carboxymethyl chitosan was prepared following the method where chitosan (10 g), sodium hydroxide (13.5 g) and solvent isopropanol (100 ml) were suspended in a flask to swell and alkalize at room temperature for 1 h. The monochloroacetic acid (15 g) was dissolved in isopropanol and was added to the reaction mixture drop wisely within 30 min and reacted for 4 h at 55°C. Then the reaction was stopped and isopropanol was discarded. Ethyl alcohol (80%) was added and the solid product was filtered and rinsed with 80–90% ethyl alcohol to desalt and dewater, and vacuum dried at 50°C (Mohamed, R.R. *et al.,* 2014).

2.4 Characterization of Carboxymethyl Chitosan
2.4.1 Fourier Transform Infrared (FTIR) and Nuclear Magnetic Resonance (NMR) Study

The FTIR spectra of chitosan and the Carboxymethyl chitosan were recorded on (Agilent

Cary 630) by the KBr pellet method in the wavelength region between 4000 to 400 cm^{-1}.

The formation of Carboxymethyl chitosan was confirmed by NMR study. Carboxymethyl chitosan was characterized by ^{13}C NMR (Bruker AVANCE, FT-NMR spectrophotometer, deuterium oxide solvent) (Tzaneva, D. *et al.,* 2017).

2.5 Oxidized alginate Preparation
Oxidized sodium alginate (OA) was prepared according to a previously reported method with some modification. Briefly, 100 ml solution of 1% (w/v) sodium alginate (0.8 g, 4.04 mmoluronate) in ethanol solution was prepared. The solution was mixed with aqueous solution containing various specified concentrations of sodium periodate at room temperature. The concentrations were calculated according to molar ratio of (sodium periodate/urinate) which was selected as 0.1, 0.3, and 0.5 to have OA with a different oxidation degree. The mixing was continued for 6 h in the dark to avoid any undesirable reactions. In order to stop oxidation reaction, ethylene glycol was added to the system and stirring was continued for 30 min. The prescribed amount of sodium chloride and ethanol were added while the system was under stirring. After 15 min, the precipitates were collected by a centrifuge (2000 rpm) and re-dissolved in distilled water (100 ml). The prescribed amount of sodium chloride and ethanol was added again to the system and after 15 min stirring, the precipitates were isolated by a centrifuge, dried by vacuum, and kept in a refrigerator prior to use (Baniasadi, H. *et al.,* 2016)

2.6 Preparation of Heliotropium indicum extract loaded Carboxymethyl chitosan hydrogel
SLNs loaded Carboxymethyl chitosan hydrogel was prepared by a simple mixing method. Briefly, a calculated weight of SLNs containing Heliotropium indicum extract were premixed with carboxymethyl chitosan aqueous solution (40 mg/ml), followed by addition of oxidized alginate aqueous solution (40 mg/ml) to incubate at 37°C for 5 min to obtain the loaded Heliotropium indicum extract hydrogel (Li, X. *et al.,* 2012).

2.6.2 Water Vapor Transmission
For these measurements, 1 g of hydrogels samples was placed on cloth and tied as cap on the mouth of a flask with a diameter of about 26 mm containing 20 ml of distilled water. The flask was then placed in a constant temperature-humidity chamber for 72 h (37 °C at 75% RH). The mass loss of the system was considered as an index of water vapour transmission rate (WVTR). The WVTR (g/m^2/h) of each sample was calculated by using the following equation.

$$WVTR\left(\frac{g}{m2}{h}\right) = \frac{M_0 - M_1}{72 \times A} 10^6$$

Where A is the area of flask mouth (mm^2), M_0 and M_1 are the mass of the system (flask and hydrogel cap) before and after placing in the chamber, respectively (Hurler, J. *et al.,* 2016; Balakrishnan, B. *et al.,* 2005).

2.6.3 Rate of Evaporation of Water
For measurement of rate of evaporation of water exactly 1 g of hydrogel sample (in triplicate) was kept at 37 °C and 75% RH. After 72 h the weight was noted (Zhao, L. *et al.,* 2013). Weight percentage was found out by the equation:

$$Weight remaining(\%) = \frac{W_t}{W_0} \times 100$$

Where W_0 and W_t are initial weight and weight after time 't' respectively.

2.7 Evaluation of Wound Healing Activity
The experimental protocol was approved by institutional animal ethical committee as per guidelines issued by Committee of Purpose of Control and Supervision of Experiment on Animals (CPCSEA) India.

Animals
Male albino wistar rats (150-200g) were used for study. All animals had free access to pelleted food and water *ad libitum*. Temperature was maintained at 23± 1ºC.

Treatment
Animals were wounded under low dose ether anaesthesia, semi aseptically. The animals were assigned into Six groups (n=6). Group I was untreated group, this was taken as Normal. Group II animals received ointment base treatment. Group III animals received marketed Fucidin ointment treatment, while group of IV received test formulation I (Heliotropium indicum extract NP-Hydrogel). No other topical or systemic therapy was given to animals during the course of this study.

Excision wound model
Hair was removed from dorsal thoracic central region of anaesthetized rats. Full thickness from the demarked area was excised to produce wound measuring around 180 mm^2. Wound was cleaned with cotton swab soaked in alcohol. The two test formulations, ointment base and marketed Fucidin ointment were applied on wound once daily for 21 days starting from the first day of inducing the wound. Wound contraction was measured for 21 days at interval of 3 days (Patel, M. *et al.,* 2013).

3. RESULTS AND DISCUSSION

3.1 Particle size Zeta potential and SEM

The average particle size results showed that the nanoparticle size of N2 was in the range of 0.4-0.8 µm and polydispersivity index less than 1 (Figure 1). Zeta potential was determined by Zetasizer and all the formulations showed a negative value and the value was in the range of -33.2 ± 0.5 to -39.2 ± 0.1, indicating better stability and less chances of aggregation of particles (Table 2).

3.2 Fourier Transform Infrared (FTIR) and Nuclear Magnetic Resonance (NMR) Study

FTIR spectra of chitosan shows bands at 3455 and 3428 cm^{-1} corresponding to the –NH2 group, while the spectra of carboxymethyl chitosan shows a strong peak at 1412 cm^{-1} due to symmetrical COO− group stretching vibration (Figure 2). Also the C–O absorption peak of the secondary hydroxyl group became stronger and was shifted to 1078 cm^{-1}which indicated that the carboxymethylation process had occurred at the C6 position of chitosan.

The ^{13}C NMR of chitosan showed peaks at 177.9 ppm and at 25 ppm, which are assigned to the carbonyl carbon of –COCH$_3$ and the methyl carbon (–CH$_3$). The signal at 101.3 ppm is assigned to the hydrogen bonded to carbon of chitosan and the signals in 59.6 ppm, 73.1 ppm, 81.1 ppm, 78.6 ppm, and 64 ppm are assigned to carbons of glucopyranose (Figure 3&4). . The ^{13}C NMR of carboxymethyl chitosan showed the signal shifted from 101.3 ppm to 105.9 ppm because of the electron-withdrawing effect of the carboxymethyl substituents. The signal observed at 180.7 ppm is assigned to the carbonyl carbons of carboxymethyl groups while the one detected at 177.9 ppm corresponds to the carbonyl carbon of –COCH3 of the parent chitosan. The methylene groups (–CH2), carbons give rise to the signals at 53 and 57.4 ppm, respectively. However, no signal was detected at 53 ppm in the spectrum of carboxymethyl chitosan and the weak signal at 58.4 ppm can be probably assigned to the methylene (–CH$_2$) bonded to the amino group (–NH). These features are taken as evidence that the carboxymethylation occurred at the hydroxyl as well as in the amino groups of chitosan.

3.3 Water vapor transmission and Rate of evaporation of water

The rate of water vapor transmission is an important parameter of the dressing and represents the dressing's ability to retain moisture. The water vapor permeability of a wound dressing should prevent both excessive dehydration as well as buildup of exudate. It was recommended that a rate of 2500 g/m^2 per day, which being in the mid-range of loss rates from injures skin, would provide an adequate level of moisture without risking wound dehydration. The prepared hydrogels had WVTR in the range of 2187.9 g/m^2 to 2954 g/m^2 could maintain a suitable moist environment in the wound that could enhance the wound contraction and tissue regeneration, thereby accelerating wound healing.

3.4 Evaluation of Wound Healing Activity

5 groups of 6 animals each were categorised as Normal, Control, Standard (Marketed Fucidin ointment) and Test group I (Formulated Heliotropium indicum extract SLN Hydrogel H3). The wound was induced by excise wound model and the study was carried out for 21 days with application of hydrogel once in a day. Figure 5 shows that the Heliotropium indicum extract SLN Hydrogel significantly contributed to wound healing compared with the blank control group and blank SLN Hydrogel at 15 and 18 day post-wounding ($P < 0.05$). The wound healing effects of Heliotropium indicum extract SLN Hydrogel may be attributed to the presence of phytoconstituents like alkaloids, triterpenoids, tannins and flavonoids in the extracts which are known to promote the wound healing process mainly due to their antimicrobial property. Flavonoids and triterpenoids are also known to promote the wound healing process mainly due to their astringent and antimicrobial property, which seems to be responsible for wound contraction.

4. CONCLUSION:

Solid lipid nanoparticles with glycerol tristearate as encapsulating matrix of Heliotropium indicum, in hydrogel of carboxymethyl chitosan and oxidised sodium alginate was prepared in view of a potential wound dressing with enhanced healing efficacy. Nanoparticle containing Heliotropium indicum extract could be released slowly from Carboxymethyl chitosan oxidized alginate hydrogel hydrogel in a sustained manner to stimulate fibroblast proliferation, capillary formation and collagen production that can significantly effect on the healing phases. As a result, we suggested that the prepared hydrogel might have great potential application in the wound healing.

Table 1: Nanoparticle composition and entrapment efficiency

| Formulation	Glycerol tristearate (mg)	Heliotropium indicum extract (mg)	Poloxamer 188 (%)
N1	300	20	3
N2	300	30	3
N3	300	30	2
N4	200	20	3
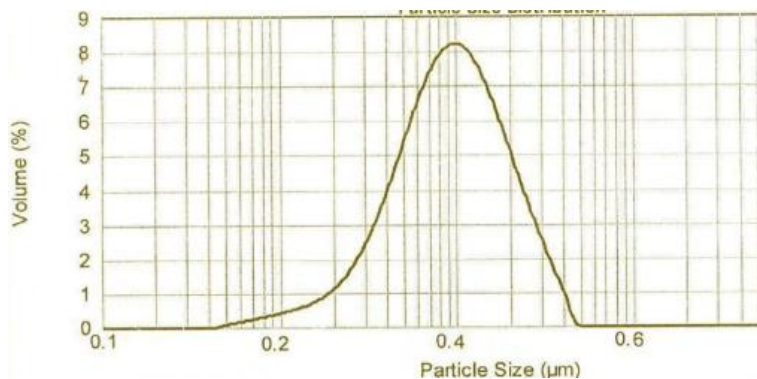
Figure 1: Particle size distribution of N2

Table 2: Zeta potential values of different Nanoparticle formulation

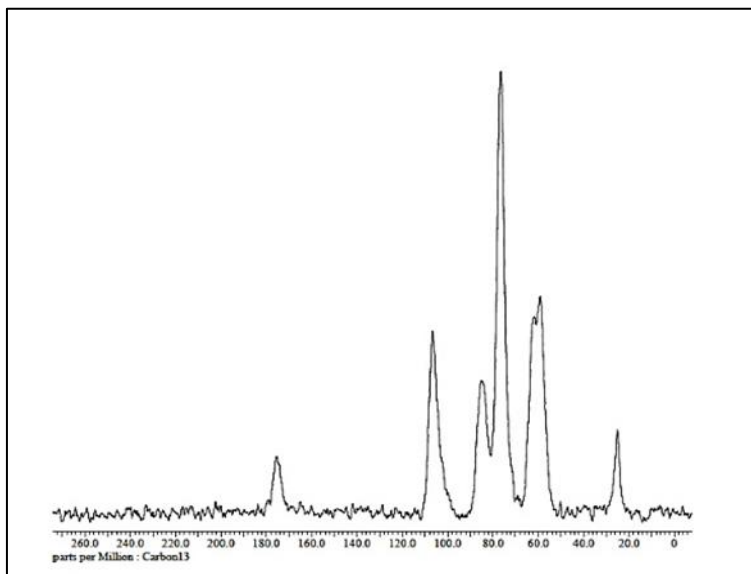| Nanoparticle code	Zeta Potential (mv)
N1	-36.7□0.8
N2	-37.6□0.2
N3	-39.2□0.1
N4	-33.2±0.5
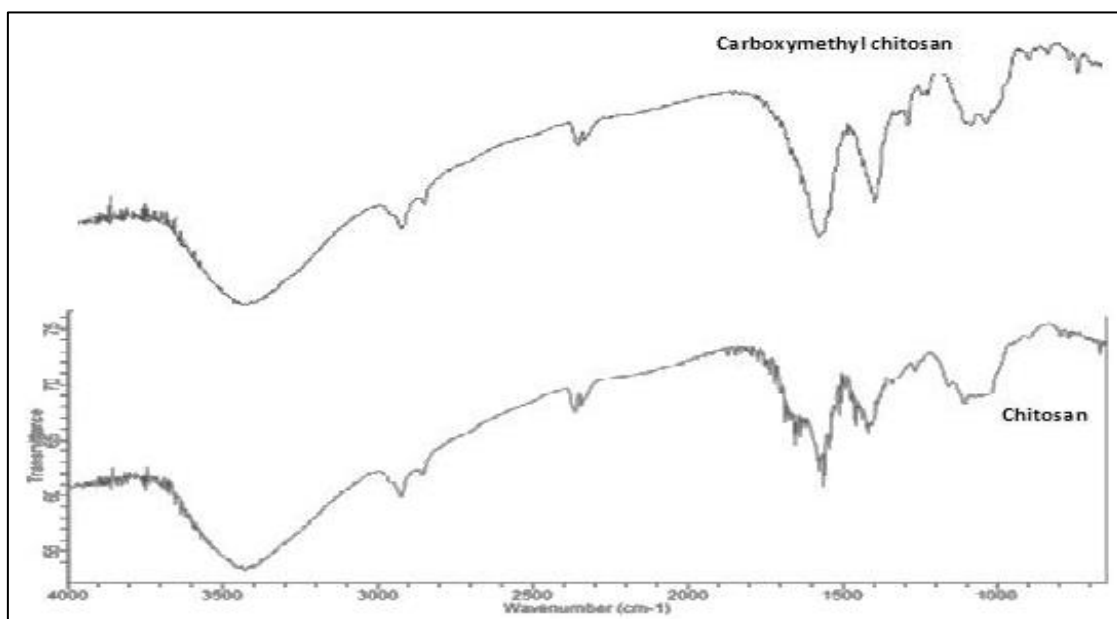
Figure 2: FTIR of Chitosan and carboxymethyl chitosan
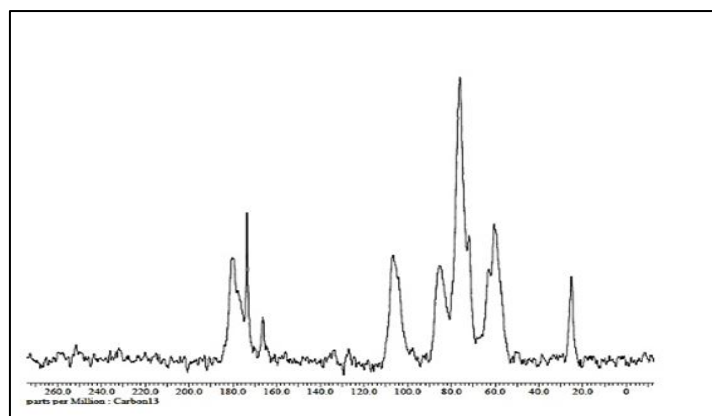
Figure 3: Nuclear Magnetic Resonance of Chitosan

Figure 4: Nuclear Magnetic Resonance of Chitosan

Table 3: Heliotropium indicum extract loaded Carboxymethyl chitosan hydrogel

Ingredients	F1	F2	F3	F4
Heliotropium indicum extract (**N2**)	50 mg	100 mg	200 mg	100 mg
Carboxymethyl chitosan	200 mg	200 mg	200 mg	160 mg
oxidized alginate	200 mg	200 mg	200 mg	240 mg
Purified Water Qs to make	10 g	10 g	10 g	10 g

Table 4: Water vapor transmission rate values of hydrogels

Type of hydrogel	WVTR (g/m^2 per day)
H1	2337.70±538.4
H2	2835.18±674.8
H3	**2187.9±578.3**
H4	2954.2±442.5

Groups	Treatment	Days			
		0	12	15	21
I	Normal				
II	Control				

III	Standard			Completely Healed	Completely Healed
IV	Test group I				
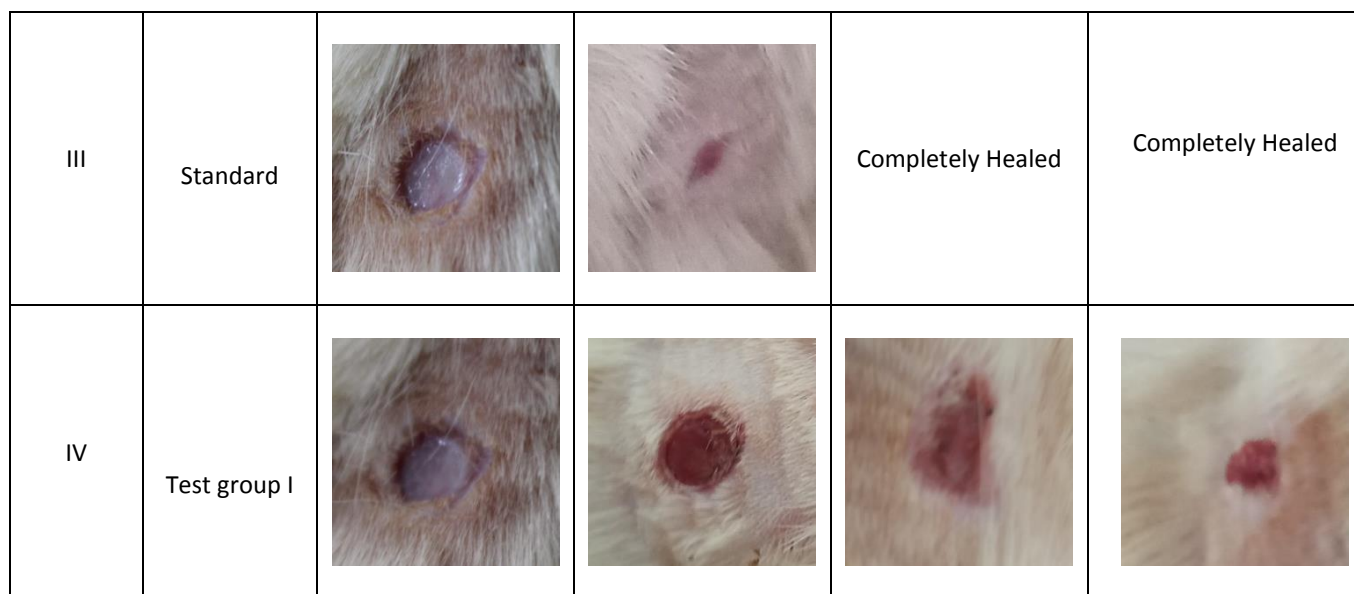
Figure 5: In vivo wound healing studies of the hydrogels containing Heliotropium indicum extract nanoparticles

Table 5: Wound Area measurement of four groups for 21 days

	Wound Area (mm^2)			Test Group I (Group IV)
	Normal	**Control**	**Standard**	
Post wounding days	**(Group I)**	**(Group II)**	**(Group III)**	
0	0	184 ± 17.23	197 ± 15.28	195 ± 18.98
3	0	173 ± 6.9	158 ± 8.18	177 ± 7.91
6	0	169 ± 7.6	110 ± 8.87	167 ± 8.58
9	0	164 ± 5.45	55 ± 8.31	157 ± 9.67
12	0	158 ± 6.47	20 ± 7.19	129 ± 8.21
15	0	154 ± 7.32	0	107 ± 6.67
18	0	152 ± 5.37	0	87 ± 5.1
21	0	147 ± 6.6	0	59 ± 3.29

REFERENCES:

1. Abbas, M., Hussain, T., Arshad, M., Ansari, A. R., Irshad, A., Nisar, J., ... & Iqbal, M. (2019). Wound healing potential of curcumin cross-linked chitosan/polyvinyl alcohol. *International journal of biological macromolecules*, *140*, 871-876.

2. Balakrishnan, B., Mohanty, M., Umashankar, P. R., & Jayakrishnan, A. (2005). Evaluation of an in situ forming hydrogel wound dressing based on oxidized alginate and gelatin. *Biomaterials*, *26*(32), 6335-6342.

3. Baniasadi, H., Mashayekhan, S., Fadaoddini, S., & Haghirsharifzamini, Y. (2016). Design, fabrication and characterization of oxidized alginate–gelatin hydrogels for muscle tissue engineering applications. *Journal of biomaterials applications*, *31*(1), 152-161.

4. Chen, L., Tian, Z., & Du, Y. (2004). Synthesis and pH sensitivity of carboxymethyl chitosan-based polyampholyte hydrogels for protein carrier matrices. *Biomaterials*, *25*(17), 3725-3732.

5. Chen, X. G., & Park, H. J. (2003). Chemical characteristics of O-carboxymethyl chitosans related to the preparation conditions. *Carbohydrate Polymers*, *53*(4), 355-359.

6. Chen, X. G., & Park, H. J. (2003). Chemical characteristics of O-carboxymethyl chitosans related to the preparation conditions. *Carbohydrate Polymers*, *53*(4), 355-359.

7. Chen, X. G., Wang, Z., Liu, W. S., & Park, H. J. (2002). The effect of carboxymethyl-chitosan on proliferation and collagen secretion of normal and keloid skin fibroblasts. *Biomaterials*, *23*(23), 4609-4614.

8. Domard, A., Rinaudo, M., & Terrassin, C. (1986). New method for the quaternization of chitosan. *International Journal of Biological Macromolecules*, *8*(2), 105-107.

9. Dreifke, M. B., Jayasuriya, A. A., & Jayasuriya, A. C. (2015). Current wound healing procedures and potential care. *Materials Science and Engineering: C*, *48*, 651-662.

10. Hurler, J., Engesland, A., Poorahmary Kermany, B., & Škalko-Basnet, N. (2012). Improved texture analysis for hydrogel characterization: gel cohesiveness, adhesiveness, and hardness. *Journal of Applied Polymer Science*, *125*(1), 180-188.

11. Hynes, R. O. (2009). The extracellular matrix: not just pretty fibrils. *Science*, *326*(5957), 1216-1219.

12. Jacob, B., Sindhu, R., Manipal, S., Prabu, D., Mohan, R., & Bharathwaj, V. V. (2019). Effectiveness of Chitosan on Oral Wound Healing: A Systematic Review. *Journal of Pharmaceutical Sciences and Research*, *11*(10), 3451-3457.

13. Li, X., Chen, S., Zhang, B., Li, M., Diao, K., Zhang, Z., ... & Chen, H. (2012). In situ injectable nano-composite hydrogel composed of curcumin, N, O-carboxymethyl chitosan and oxidized alginate for wound healing application. *International journal of pharmaceutics*, *437*(1-2), 110-119.

14. Liu, Q., Huang, Y., Lan, Y., Zuo, Q., Li, C., Zhang, Y., & Xue, W. (2017). Acceleration of skin regeneration in full-thickness burns by incorporation of bFGF-loaded alginate microspheres into a CMCS–PVA hydrogel. *Journal of tissue engineering and regenerative medicine*, *11*(5), 1562-1573.

15. Lu, G., Kong, L., Sheng, B., Wang, G., Gong, Y., & Zhang, X. (2007). Degradation of covalently cross-linked carboxymethyl chitosan and its potential application for peripheral nerve regeneration. *European Polymer Journal*, *43*(9), 3807-3818.

16. Martin, P. (1997). Wound healing--aiming for perfect skin regeneration. *Science*, *276*(5309), 75-81.

17. Merisko-Liversidge, E., McGurk, S. L., & Liversidge, G. G. (2004). Insulin nanoparticles: a novel formulation approach for poorly water soluble Zn-insulin. *Pharmaceutical research*, *21*(9), 1545-1553.

18. Min, S. K., Lee, S. C., Hong, S. D., Chung, C. P., Park, W. H., & Min, B. M. (2010). The effect of a laminin-5-derived peptide coated onto chitin microfibers on re-epithelialization in early-stage wound healing. *Biomaterials*, *31*(17), 4725-4730.

19. Mohamed, R. R., & Sabaa, M. W. (2014). Synthesis and characterization of antimicrobial crosslinked carboxymethyl chitosan nanoparticles loaded with silver. *International journal of biological macromolecules*, *69*, 95-99.

20. Patel, M., Nakaji-Hirabayashi, T., & Matsumura, K. (2019). Effect of dual-drug-releasing micelle–hydrogel composite on wound healing in vivo in full-thickness excision wound rat model. *Journal of Biomedical Materials Research Part A*, *107*(5), 1094-1106.

21. Patrulea, V., Laurent-Applegate, L. A., Ostafe, V., Borchard, G., & Jordan, O. (2019). Polyelectrolyte nanocomplexes based on chitosan derivatives for wound healing application. *European Journal of Pharmaceutics and Biopharmaceutics*, *140*, 100-108.

22. Patrulea, V., Ostafe, V., Borchard, G., & Jordan, O. (2015). Chitosan as a starting material for wound healing applications. *European Journal of Pharmaceutics and Biopharmaceutics*, *97*, 417-426.

23. Pignatello, R., Ricupero, N., Bucolo, C., Maugeri, F., Maltese, A., & Puglisi, G. (2006). Preparation and characterization of eudragit retard nanosuspensions for the ocular delivery of cloricromene. *Aaps Pharmscitech*, *7*(1), E192-E198.

24. Rodrigues, M., Kosaric, N., Bonham, C. A., & Gurtner, G. C. (2019). Wound healing: a cellular perspective. *Physiological reviews*, *99*(1), 665-706.

25. Shah, M., & Agrawal, Y. (2012). Ciprofloxacin hydrochloride-loaded glyceryl monostearate nanoparticle: Factorial design of Lutrol F68 and Phospholipon 90G. *Journal of microencapsulation*, *29*(4), 331-343.

26. Sieval, A. B., Thanou, M., Kotze, A. F., Verhoef, J. C., Brussee, J., & Junginger, H. E. (1998). Preparation and NMR characterization of highly substitutedN-trimethyl chitosan chloride. *Carbohydrate Polymers*, *36*(2-3), 157-165.

27. Sultankulov, B., Berillo, D., Sultankulova, K., Tokay, T., & Saparov, A. (2019). Progress in the development of chitosan-based biomaterials for tissue engineering and regenerative medicine. *Biomolecules*, *9*(9), 470.

28. Tzaneva, D., Simitchiev, A., Petkova, N., Nenov, V., Stoyanova, A., & Denev, P. (2017). Synthesis of carboxymethyl chitosan and its rheological behaviour in pharmaceutical and cosmetic emulsions. *Journal of Applied Pharmaceutical Science*, *7*(10), 070-078.

29. Upadhyaya, L., Singh, J., Agarwal, V., & Tewari, R. P. (2013). Biomedical applications of carboxymethyl chitosans. *Carbohydrate polymers*, *91*(1), 452-466.

30. Zhao, L., Zhu, B., Jia, Y., Hou, W., & Su, C. (2013). Preparation of biocompatible carboxymethyl chitosan nanoparticles for delivery of antibiotic drug. *BioMed research international*, *2013*.

31. Zhu, X., Chian, K. S., Chan-Park, M. B. E., & Lee, S. T. (2005). Effect of argon-plasma treatment on proliferation of human-skin–derived fibroblast on chitosan membrane in vitro. *Journal of Biomedical Materials Research Part A: An Official Journal of The Society for Biomaterials, The Japanese Society for Biomaterials, and The Australian Society for Biomaterials and the Korean Society for Biomaterials*, *73*(3), 264-274.